

# Investigation of the Small Pixel Effect in CdZnTe Detectors

Matthew D. Wilson, Paul Seller, *Member, IEEE*, Matthew C. Veale & Paul J. Sellin *Member, IEEE*

**Abstract**—The signal shapes produced by alpha and X-ray radiation in 2mm thick CdZnTe detectors have been measured. The signals produced in a single large pad detector and a 300 $\mu$ m pixilated detector have been compared. The influence of the small pixel effect and its variation with detector bias is visible. Synopsys Sentaurus TCAD is used to simulate the charge carrier motion in the detectors and is compared against the measured signals. A description of how the simulations will aid detector design with optimal pixel size, inter-pixel spacing and bias voltage is included

## I. INTRODUCTION

CADMIUM Zinc Telluride (CdZnTe) is used as a high energy X-ray detector conversion material to achieve both fine spatial imaging and good spectral resolution. CdZnTe X-ray detector performance is limited by low hole mobility and poor carrier lifetimes. There are several ways to circumvent the poor transport properties of holes such as bi-parametric correction [1][3], coplanar electrodes [2][3], Frisch grids [3] and the small pixel effect [3][4]. The detector used in this investigation makes use of the small pixel effect. The small pixel effect can be conceptualized using the Shockley-Ramo theorem [5] [6]. The weighting field that surrounds a small pixel is only of considerable magnitude close to the pixel. Therefore charge carriers will only induce a significant signal on a pixel when they are in close proximity to the pixel. In 2mm thick CdZnTe detectors, irradiated at the cathode, the charge carriers will be generated within the first few hundred micrometers, far from the pixel array anodes. The holes will drift to the cathode without inducing a significant signal on a pixel. The signal is practically induced exclusively by electrons and the problems posed by poor hole transport properties are negated. As the signal is induced by electrons drifting near to the pixels, as opposed to drifting through the entire bulk of the material, the signals from small pixel detectors will have a faster signal rise-time than pad detectors.

This gives an additional benefit in small pixel detectors by allowing faster analogue readout without ballistic deficient effects.

Understanding the extent of the weighting field, its effect on the suppression of induced charge due to carrier drift in the bulk, and the exact electron induced signal rise-time is complicated by several factors. The photon conversion produces a photoelectron and fluorescent X-ray that give a significant size to the initial charge carrier cloud [7]. As the charge carrier cloud drifts through the material the cloud diffuses. In a simple system the charge cloud would obey Einstein's diffusion equation [8] and expand uniformly in all directions. In a biased detector the internal electric field perturbs the energy distribution of the charge carriers. The charge carriers diffuse with a diffusion constant that is a function of bias field. The diffusion parallel to bias field is greater than diffusion perpendicular to the bias field [9] [10]. The eventual width of the cloud, perpendicular to the bias field has a strong influence on the probability of charge sharing events in small pixel detectors. The length of the charge cloud, parallel to the bias field, limits the rise-time of the induced signals and must be considered in analogue readout design.

A potential limitation of small pixel detectors is charge sharing, which is detrimental to the energy resolution of the detector. In this investigation 2mm thick CdZnTe detectors with 300 $\mu$ m pixels are examined. Charge sharing events are frequent with this detector geometry because the charge carrier cloud widths are comparable to the pixel size. The correct signal magnitude is regained by adding the nearest neighbor signals together.

The small pixel effect is investigated by examination of the signals induced on the pixels. Interpretation of the signal shapes is complicated as the shape and duration of the signals are dependent on a number of factors such as the extent and profile of the weighting fields, the shape of the charge carrier cloud before and after drift and diffusion through the bulk. In order to gain a greater understanding of the signal shapes the detector is simulated using a Technology Computer Aided Design (TCAD) package from Synopsys. The TCAD package allows the user to construct any design of detector, produce electron-hole pairs at any position in the detector, observe the drift, diffusion and interaction of the charge carriers and the signals that they induce on the pixels. A direct comparison between the experimental and simulated signals allows the experimental signal shapes to be explained in terms of real phenomena within the detector. Not only does the TCAD

---

THIS IS A PRE-PRINT COPY. This work was conducted as part of the HEXITEC collaboration. HEXITEC is funded by the EPSRC, UK.

M. D. Wilson is with the Science and Technology Facilities Council, Rutherford Appleton Laboratory, Oxfordshire, OX11 0QX, UK (telephone: +44 (0) 1235 44 5313, e-mail: Matt.Wilson@stfc.ac.uk).

P. Seller is with the Science and Technology Facilities Council, Rutherford Appleton Laboratory, Oxfordshire, OX11 0QX, UK (telephone: +44 (0) 1235 44 6850, e-mail: p.seller@stfc.ac.uk).

M. C. Veale is with the Physics Department, University of Surrey, Guildford, Surrey, GU2 7XH, UK (telephone: 44 (0) 1483 876814, email: M.Veale@surrey.ac.uk)

P. J. Sellin is with the Physics Department, University of Surrey, Guildford, Surrey, GU2 7XH, UK (telephone:+44 (0) 1483 876814, email: P.Sellin@surrey.ac.uk)

software improve the understanding of current detectors but it is a valuable tool in designing new devices.

## II. EXPERIMENTAL EQUIPMENT AND TECHNIQUE

The detector used in this investigation was a 2mm thick CdZnTe purchased from eV Products. The anode of the detector was a 16x16 matrix of 300x300 $\mu$ m pixels. The pixels were bump bonded to a MAC04 ASIC containing a pre-amplifier for each of the 256 pixels. The signal from a single pixel was buffered and digitized by a XIA PIXIE-4 Digital Gamma Finder. The digitized signal shapes were normalized to allow averaging of the signals to increasing the signal to noise ratio and to give easier comparison between different magnitudes of signal. A software program was used to extract the signal rise-time measurements (10-90%). Fig 1 shows a schematic of the data acquisition system used to capture the signal shapes.

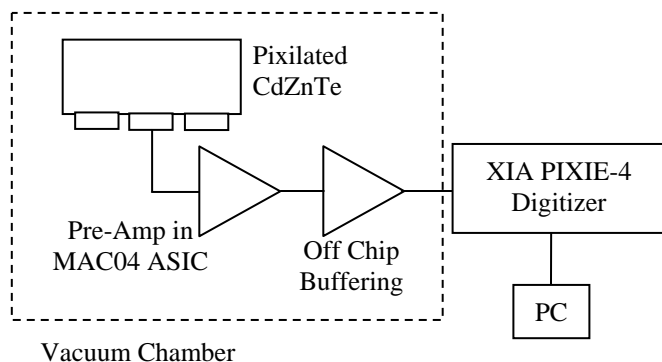


Fig 1. A schematic of the experimental apparatus. The cooled CdZnTe is held in a vacuum chamber. The signal from a pixel on the CdZnTe sample is amplified by a MAC04 ASIC and is routed out to off-chip buffering electronics. The signal is then digitized by a XIA PIXIE-4 Digital Gamma Finder and sent into a PC for analysis.

## III. EXPERIMENTAL RESULTS

### A. Comparison to a Pad Detector

To illustrate the small pixel effect the pixilated detector was directly compared to a 3x3mm pad CdZnTe detector made from 2mm thick eV Products material. The signals from the pad detector were amplified using an AmpTek A250 preamplifier, digitized with a XIA Polaris digital gamma spectrometer and processed in the same manner. An Am-241 alpha source was used to irradiate the pad and pixilated devices so that all of the charge carriers were created in a small region close to the cathode. Fig 2 shows the signal shape for the pad and pixilated detectors with a bias of -100V at room temperature (295K). The 10-90% signal rise-time for the pad and pixilated detectors was 590ns and 227ns respectively. The pixilated detector has a quicker signal rise-time because of the small pixel effect. The charge carriers in the pad detector induce a signal on the 3mm collecting contact throughout the entire drift across the 2mm detector.

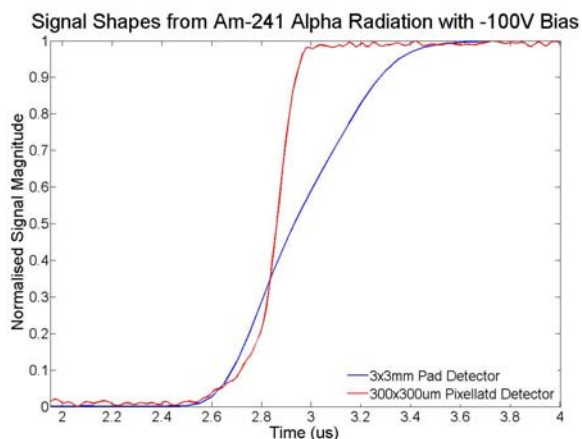


Fig 2. Signal shapes from Am-241 alpha radiation for the 3x3mm pad and pixilated detector. The faster rising signal is from the pixilated detector and the slower rising signal is from the pad detector.

The signal shape from the pad detector in Fig 2 shows a long rising signal with a constant gradient for the majority of the signal. This is directly related to the weighting potential in the pad detector which is linear between the anode and cathode. The curvature at the top of the pad detector signal is not a feature of the weighting field but is due to the lower charge density tail of the charge carrier cloud. Evidence to support this is presented later and is illustrated in Fig 5. The signal shape from the pixilated detector in Fig 2 has similar features. The rising edge of the signal shape is due to the lower charge density front of the charge carrier cloud entering the small pixel weighting field. The signal rises linearly in the middle of the pixel as the bulk of the charge carrier cloud drift through the high weighting field. The curvature at the top of the signal shape is due to the lower charge density tail in the charge carrier cloud.

### B. Pixilated Detector Signal Shapes

The pulse shapes from an Am-241 alpha source and X-rays from a Tb fluorescence source were compared using the pixilated detector. The alpha and X-ray radiation generates charge carriers far from the small pixels in 2mm thick CdZnTe. The signal shapes induced on the small pixel detector will be from the charge carrier cloud after a significant drift and diffusion. Fig 3 shows the signal shapes generated by alpha particles and X-rays in the pixilated detector with a bias of -100V and -300V. For a relatively low bias of -100V the signal from alpha exposure is significantly slower than that from X-ray exposure. At -300V the signal shapes are more similar in shape and duration.

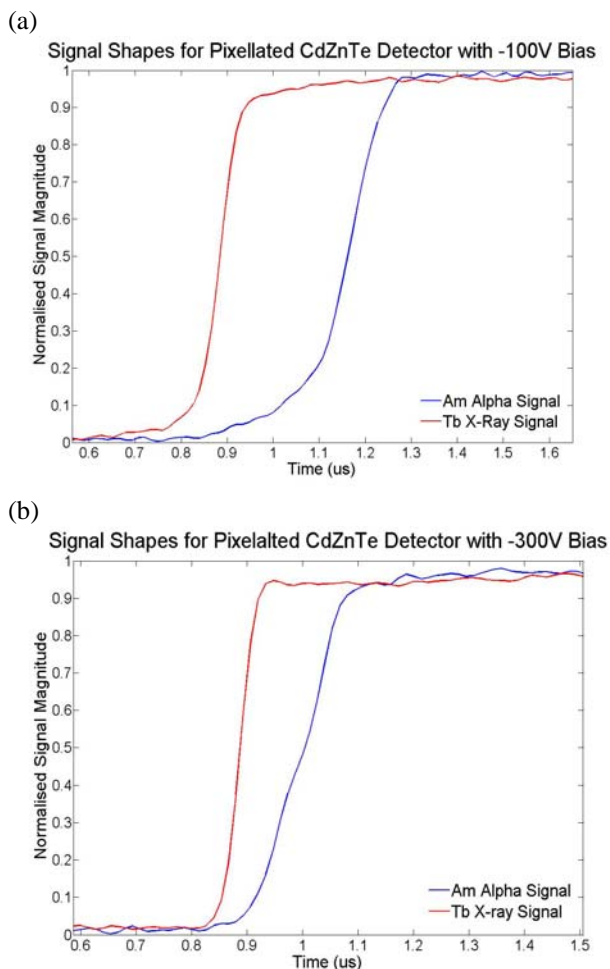


Fig 3. The signal shapes from Am-241 alpha particles and Tb fluorescence source X-rays for (a) -100V and (b) -300V applied to the pixelated detector. The signal shapes from the Tb X-rays are the faster rising signals.

The reason for the observed difference between alpha-particle and X-ray signals is due to the larger charge carrier density that alpha particle interactions generate. The larger densities of positive and negative charge carrier clouds results in an increased attraction between the two clouds when they are in close proximity. The attraction causes the charge carrier clouds to be elongated as they drift apart under the bias field. The longer charge carrier cloud takes a longer time to drift through the high weighting field region, inducing a slower signal shape. The interaction between oppositely charged carrier clouds becomes less pronounced with increasing bias as the charge carrier clouds to separate more rapidly. The charge carrier densities created by X-ray interactions are sufficiently small to reduce this effect to an insignificant amount. The variation in the signal shape rise-times for alpha and X-ray exposure is plotted in Fig 4. The rise-times for alpha particle exposure are significantly slower when the applied bias is low and tends towards the X-ray signal rise-times for high bias magnitudes. The TCAD simulations are consistent with experiment, as shown in Fig 5. The evolution of the negative charge carriers shows a number of effects. The large charge carrier diffusion parallel and perpendicular to the

field is evident. The lower carrier density at the front of the cloud reaches the high weighting field first. This is the cause of the curved rising edge in the signal shapes from the pixelated detector. The tail of the charge carrier cloud has a lower charge density and is elongated by the attraction to the positive charge carriers (not shown here). This feature in the charge carrier cloud causes the curved end to the signal shapes in the pad and pixelated detectors.

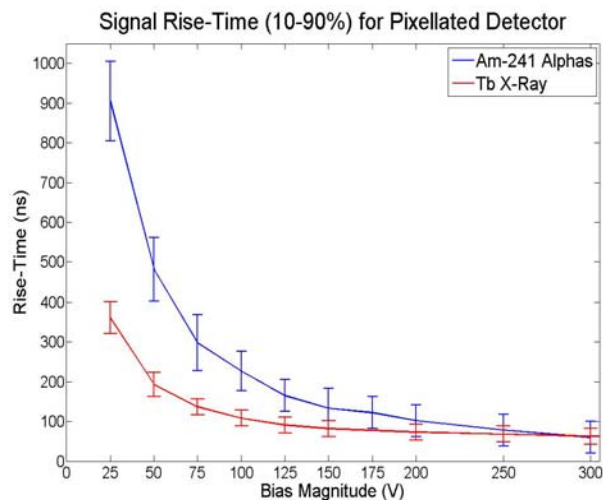


Fig 4. The signal rise-time (10% to 90%) for the pixelated detector when exposed to Am-241 alpha particles (top) and Tb X-rays (bottom).

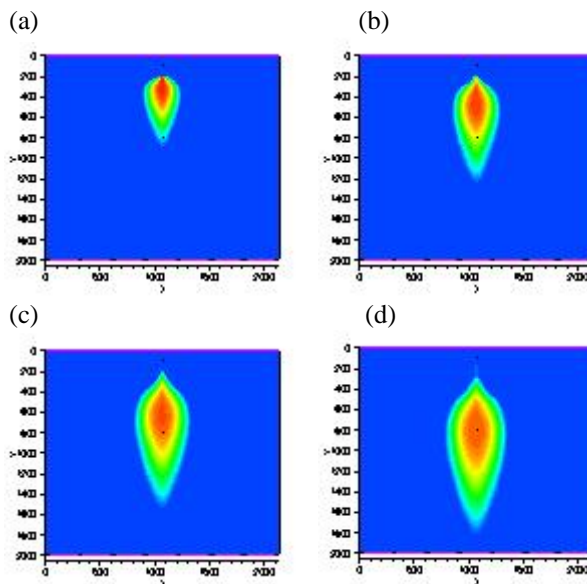


Fig 5. TCAD simulation of a 2D 2mm thick CdZnTe detector with 7 pixels, 250μm in length with 50μm spacing. A bias of - 300V was applied to the top contact. The charge generation is a model of that from a Tb X-ray. The images are of the electron density at times of (a) 10ns, (b) 20ns, (c) 30ns and (d) 40ns after the charge was generated.

#### IV. SPECTRAL RESOLUTION IMPROVEMENTS DUE TO CHARGE SHARING CORRECTIONS

In order to capture an energy spectrum a 2mm thick eV Products CdZnTe crystal with a 16x16 array of 300μm pixels was used in an ERD2004 detector system, a newer version of

the ERD system [11]. The ERD2004 system contains a MAC04 ASIC which is bump bonded to the pixels of the CdZnTe. The MAC04 is subsequently wire bonded to two SHC04 ASICs. In the ERD2004 system the signal induced on a pixel is amplified, shaped, the peak value is readout and a comparator circuit determines if the data is valid. The data extracted from the ERD2004 system gives the signal magnitude, the pixel address and timing of the signal collection. This allows subsequent data analysis to correct for charge sharing events.

TCAD simulations of the charge carrier cloud evolution were conducted. Here, the width of the charge carrier cloud is defined as the width at which the charge carrier density is greater than one standard deviation of the maximum charge carrier density. The charge carrier clouds in the TCAD simulations were observed to reach widths in excess of one hundred micrometers. The significant size of the charge carrier cloud results in a high number of charge sharing events in the pixilated detector. In order to maximize the energy resolution of the detector data processing software is used to correct the signal magnitudes of charge sharing events. The software locates a valid X-ray event on a pixel and sums the signal magnitudes of that pixel and the nearest neighboring pixels to reconstruct the full signal magnitude.

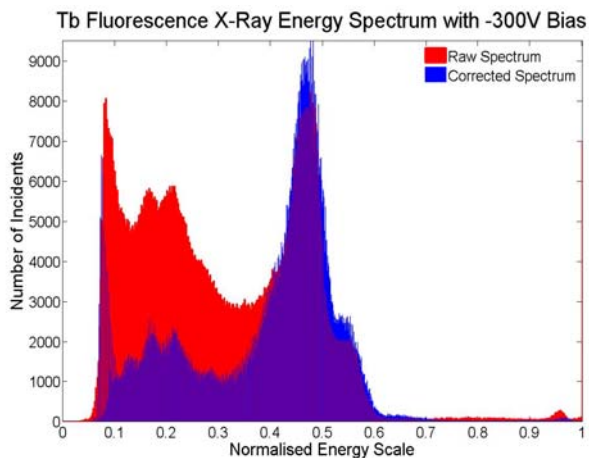


Fig 6. The energy spectrum of Tb fluorescence X-rays before and after charge sharing correction. Recorded at 273K with a bias of -300V. The energy spectrum with the lower number of low energy events is the spectrum after charge sharing correction.

Fig 6 shows the energy spectrum from a Tb X-ray fluorescence source with -300V bias before and after the charge sharing correction. The main peak is the Tb k-alpha fluorescence which is at an energy of 44.5keV. The energy spectrum has the characteristic features of charge sharing events. The main energy peak has a low energy tail and there are a large number of low energy events in the spectrum. The charge sharing correction algorithm successfully corrects for the majority of the low energy events. The resolutions of the energy peaks are not significantly improved. No events are recorded at very low energies as the ERD2004 ASICs have a

low energy threshold. Charge sharing events within this low energy range are required to correct the charge sharing events on the low energy tail of the energy peaks. A new HEXITEC ASIC will allow low energy charge sharing events to be captured and used in the correction algorithm.

## V. SIMULATIONS

The CdZnTe detectors were simulated by a commercial TCAD package from Synopsys. Sentaurus Structure Editor was used to build and mesh a detector device. Numerical simulations were conducted by Sentaurus Device. The simulation tool creates the electric field in the device from the applied bias, the pixel geometry and doping profile. In the simulations phenomenological expressions for the electron and hole mobility and diffusion constants as functions of electric field are used. The resultant expression for the current density is coupled with continuity equations for electrons and holes as well as Poisson's equation. This non-linear system of equations is discretized using the Box-Integration approach and is subsequently solved using the Newton method [12].

A two dimensional model of the pixilated device was created and simulated. The pixilated device was 2mm thick with 300 $\mu$ m pitch pixels. The mobility of the CdZnTe was specified as 1114 $cm^2/Vs$  [13] and the dielectric constant, band gap and electron affinity were set to the values as quoted by eV Products [14]. Charge was generated to model X-ray charge generation and the simulation calculated the subsequent charge carrier drift and diffusion. The signals generated on the pixels and visualization of electric fields, potential and charge carriers were recorded for analysis. Fig 7 shows an example of the signal shapes for the pixilated detector and TCAD simulation for Tb fluorescence X-ray exposure with a bias of -100V and -300V.

The main difference between the experimental and simulated signal shapes is the linear, steeper gradient rising edge to the simulated data. This is clearly visible in the -100V data. The effect is present in the -300V data but is less visible as the signal rises faster. Apart from this effect the signal shapes are in good agreement.

The origin of this disagreement in the signal rising edge is attributed to two effects. The doping and trapping profile of the CdZnTe is not accurately simulated. The resulting leakage current is unrealistic and may contribute to the linear rising edge of the signal shapes. When the charge carriers are created in the simulation it results in an instantaneous increase in the signal on the pixel. This is a software artifact not a real phenomenon.

Although better simulations are in progress it is already clear that they have the potential to be a potent tool in the understanding of existing detectors and the design of new detectors. The priority for improved simulations is to create more realistic CdZnTe material with realistic dopant and trap profiles. Additional computer processing would allow

simulations with finer mesh structures, smaller time steps and three dimensional geometries

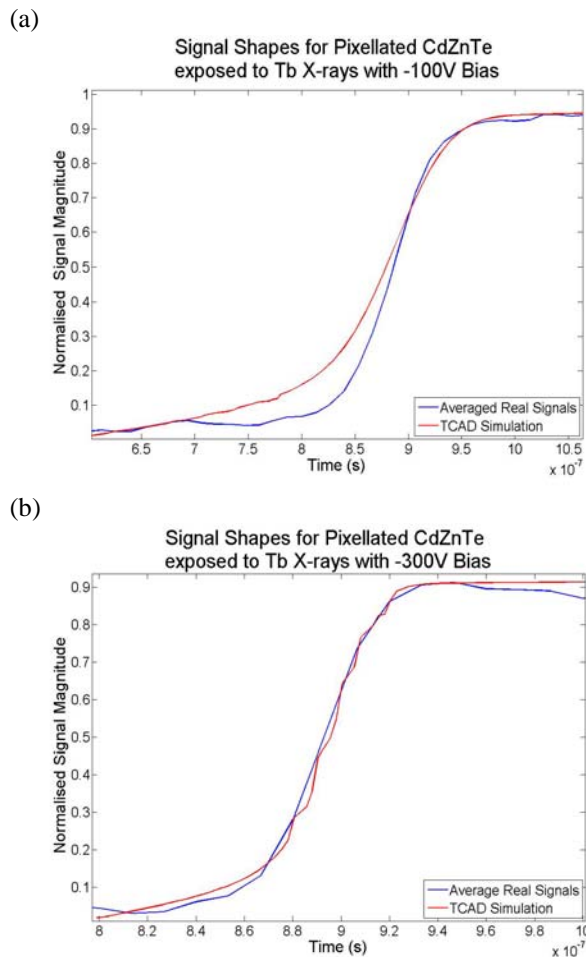


Fig 7. The signal shapes from a Tb X-ray from experimental and simulated data for a bias of (a) -100V and (b) -300V. The signal shapes from the simulation package are distinguishable by the steeper, linear rising edge of the signals.

## VI. CONCLUSION

This investigation has demonstrated the small pixel effect in 2mm thick CdZnTe detectors by observations of the induced signal shapes from alpha and X-ray radiation. TCAD simulation software has been used in direct comparison to experimental data to allow the charge carrier motion in CdZnTe detectors to be visualised. The initial size and subsequent diffusion of charge carrier clouds are identified as a major contributor to charge sharing events in pixilated detectors.

The interaction between dense clouds of positive and negative charge carriers was used to explain the slower signal durations from alpha radiation at low bias. Further investigation is required to ensure that this effect is insignificant for higher energy X-rays.

Areas for improvement have been identified for the TCAD simulations. The current level of agreement between simulated and experimental data is very encouraging.

## ACKNOWLEDGMENT

This work is motivated and funded by the HEXITEC collaboration. This collaboration is developing materials, interconnection technology and readout for imaging CdZnTe detectors.

We thank Alec Hardie for the off-chip electronics used in this investigation. We thank Nicholas Owen for his help with the use of the Synopsys TCAD software.

## REFERENCES

- [1] A. Shor, Y. Eisen & I. Mardor, "Spectroscopy with pixilated CdZnTe gamma detectors – experiment versus theory," Nucl. Instr. And Meth. A, 458, pp47-54, 2001.
- [2] P. N. Luke, "Single-polarity charge sensing in ionizing detectors using coplanar electrodes," Appl. Phys. Lett., vol.65, no.22, pp2884-2886, 28 November 1994.
- [3] Z. He, "Review of the Shockley-Ramo theorem and its application in semiconductor gamma-ray detectors," Nucl. Instr. Meth. A, 463, pp250-267, 2001.
- [4] H. H. Barret, J. D. Eskin & H. B. Barber, "Charge Transport in Arrays of Semiconductor Gamma-Ray Detectors," Phys. Rev. Lett, vol.75, no.1, pp156-159, 3 July 1995.
- [5] W. Shockley, "Currents to Conductors Induced by a Moving point Charge," J. Appl. Phys., vol. 9, pp635-636, Oct.1938.
- [6] S. Ramo, "Currents Induced by Electron Motion", Proc. IRE. Australia, vol 27, pp584-585, Sept. 1939.
- [7] E. G. d'Aillon, J. Tabary, A. Gliere, L. Verger, "Charge sharing on monolithic CdZnTe gamma-ray detectors: A simulation study," Nucl. Instr. & Meth. A, 563, pp124-127, 2006.
- [8] B. R. Nag, *Electron Transport in Compound Semiconductors*, 1<sup>st</sup> ed., Springer-Verlag Berlin Heidelberg New York, 1980, pp210-215.
- [9] D. Chattopadhyay & B. R. Nag, "Diffusion of charge carriers in high electric fields," Proc. R. Soc. Lond. A, 354, pp367-378, 1977.
- [10] R. E. Robson, "Diffusivity of Charge Carriers in Semiconductors in Strong Electric Fields," Phys. Rev. Lett., vol.31, no.13, pp825-828, 24 September 1973.
- [11] D. P. Sharma, J. A. Gaskin, B. D. Ramset & P. Seller, "Characteristics of a fine-pixel cadmium-zinc-telluride detector," Proceedings SPIE the International Society for Optical Engineering, no.4852, pp1019-1028, 2002.
- [12] R. E. Bank, D. J. Rose & W. Fichtner, "Numerical Methods for Semiconductor Device Simulation," IEEE Transactions on Electron Devices, vol. 30, no. 9, pp1031-1041, Sept 1983.
- [13] M. C. Veale, P. J. Sellin, A. Lohstroh, A.W. Davies, J. Parkin, & P. Seller, "X-ray spectroscopy and charge transport properties of CdZnTe grown by the vertical Bridgman method", Nucl. Instr. & Meth. A, vol 576, issue 1, pp90-94, June 2007.
- [14] eV Products, CdZnTe material properties available from, "www.evproducts.com/czt.html".